P1B.1 RAINFALL CHARACTERISTICS AND KINEMATIC STRUCTURE OF A MESOSCALE CONVWCTION OBSERVED DURING THE ONSET OF SOUTH EAST ASIAN MONSOON

Jian-Jian Wang
Goddard Center for Earth Science and Technology, University of Maryland Baltimore County
Mesoscale Atmospheric Processes Branch, NASA/Goddard Space Flight Center, Greenbelt, Maryland

1. INTRODUCTION

The Asian summer monsoon starts from the onset of South East Asian Monsoon (SEAM). However, as traditional observational network is far from being adequate, the lack of observation becomes a main hamper to the research on SEAM and related physical processes. The South China Sea Monsoon Experiment (SCSMEX, Lau et al. 2000) was an international field experiment conducted in South China Sea (SCS) and surrounding areas during May—June 1998. The goal of the mesoscale program was to define the initiation, structure, evolution and dynamics of precipitation processes associated with the onset and mature phase of the SEAM. The main method to accomplish this objective was the deployment of two Doppler radars (TOGA and C-POL) to form a dual-Doppler radar analysis region (Fig. 1) in the northern SCS. Other conventional meteorological observations including rawinsonde, surface observation network, and rain gauges were also collected on the radar sites and surrounding areas.

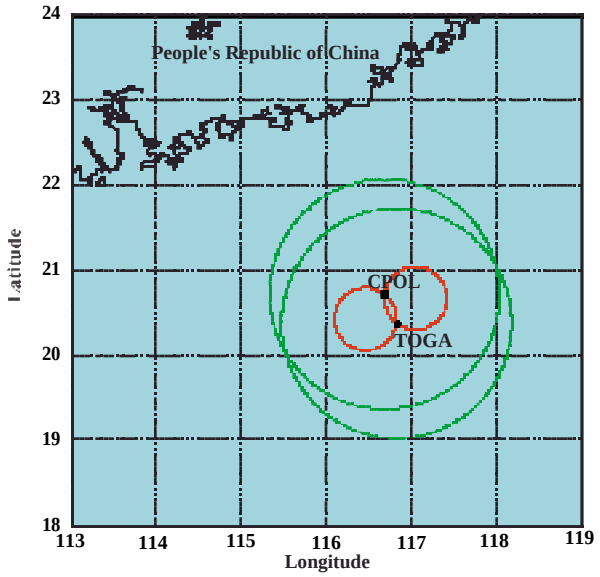

Fig. 1 Dual-Doppler radar network during SCSMEX. The big circles indicate the radar observing domain, while the small circles show the dual-Doppler radar analysis regime.

The SEAM onset in 1998 started on 15 May when two branches of tropical southwesterly airflows from Bay of Bengal and Australian region arrived the SCS area. Meanwhile, a pronounced frontal system from China entered northern SCS. Different from the frontal system reaching coastal region before SEAM onset, this system was able to enhance its intensity and areal coverage after moving into the sea. In this study, we will perform a detailed case study of 15 May to document the evolution and structure of the mesoscale convection in the SCS region for the first time. The focuses are to compare the similarities and differences among the pre- and post-frontal convection as well as the other tropical oceanic convection studied previously.

2. RAINFALL AND KINEMATIC STRUCTURE

At 0600 UTC 15 May, the main feature in the radar domain was the linear northeast to southwest oriented frontal rainband with a width of about 40 km (A in Fig. 2a). Ahead of the convective line A, there were two groups of newly formed convection at 50 km east to C-POL. The primary convective line ahead of the frontal rainband (B in Fig. 2a) was oriented north south, while the secondary convective line (B1 and B2 in Fig. 2a) was oriented east west. This was in consistent with the conclusion made by LeMone et al. (1998) from their studies on western Pacific convection when the low-level wind shear is over 4 m s^{-1}. The convection had a larger areal coverage in an hour later at 0700 UTC (Fig. 2b). However, the northeastern portion of the convection started to weaken with more stratiform characteristics from the earlier convective lines. At the same time, between the two northeast to southwest oriented convective lines and beyond, there was a tendency to form a narrow convective line (D in Fig. 2b) perpendicular to the earlier convective lines. This new line intensified and became the primary feature in the following hours. The front at 850-hPa passed the C-POL at about 0730 UTC. In the next hour, the main radar echo became an east-west oriented convective, while the dominated northeast to southwest oriented convective lines in earlier hours weakened during the same period (Fig. 2c). Weak north-south oriented lines existed to the north of main convection as the residual from the early convection. During SCSMEX, this type of sharp change of convection orientation in a time spread of several hours was frequently observed. At 0930 UTC, the north south oriented convective lines continued to dissipate with some stratiform precipitation remaining. On the contrary, the primary east-west oriented convective lines became more pronounced with enhanced intensity (Fig. 2d).

The structure of the mesoscale convection observed on 15 May (Fig. 3) shared some similarities

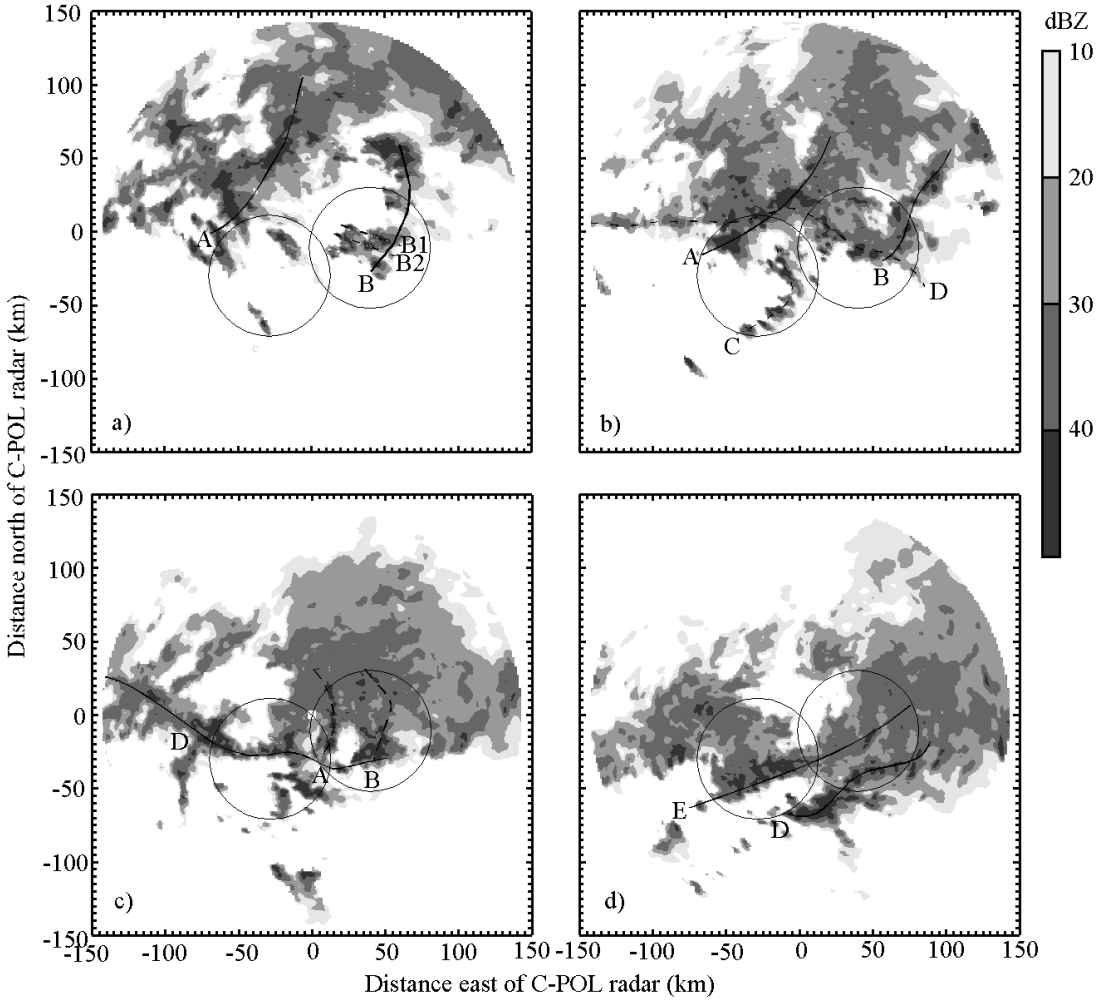

Fig. 2 CPOL radar reflectivity (dBZ) at 2.5 km MSL at (a) 0600 UTC, (b) 0700 UTC, (c) 0830 UTC, and (d) 0930 UTC, 15 May 1998.

with archetypal tropical oceanic convection documented in other geographical regions: 1) the low-level inflow from the warm and moist air ahead of the leading edge, 2) the maximum radar reflectivity at the lowest levels, 3) the strong reflectivity gradient above the 0°C isotherm implying a relative weak updraft, 4) generally an elevated (over 7.5 km MSL) vertical velocity maximum. However, significant departures were also evident: 1) a more vertical radar echo and updraft pattern with little tilt in a moderate shear environment, 2) very limited stratiform rain in an intense convection due to a very dry mid-to-upper layer resulting in a quick evaporation and sublimation, 3) a leading stratiform mode instead of the more frequent trailing stratiform mode, and 4) a maximum low-level convergence and updraft in the rear portion of the pre-frontal convection related to the more vertical convection. It is interesting to note that the kinematic structures resulting in the leading stratiform rain were different from pre-frontal to post-frontal convection. In the pre-frontal region, the leading stratiform rain was caused by a rear to front mid-level outflow blowing hydrometers forward. And, the super dry environmental air in upper levels also prevented the formation of stratiform rain there. In the post-frontal region, in contrast to most tropical convection, the low-level inflow did not go to the upper rear part of convection but turned forward at the layer above 7.5 km. Thus, the leading stratiform rain formed as a result of forward advection of the hydrometers. Please note that the stratiform rain in the right portion of Fig. 3b was not the trailing part from convective counterpart, but the residual from the pre-frontal convection.

3. STATISTICAL ANALYSIS

The contoured frequency by altitude diagrams (CFAD) is a convenient tool to display multiple histograms in a two-dimensional format. The relative frequency of occurrence of a given parameter can be shown at each height. The mean profiles and CFADs of reflectivity, system relative u- and v-component, divergence at 0620 UTC and 0930 UTC are shown in Fig. 4. The distribution and mean profile of the radar reflectivity for these convection were very identical at

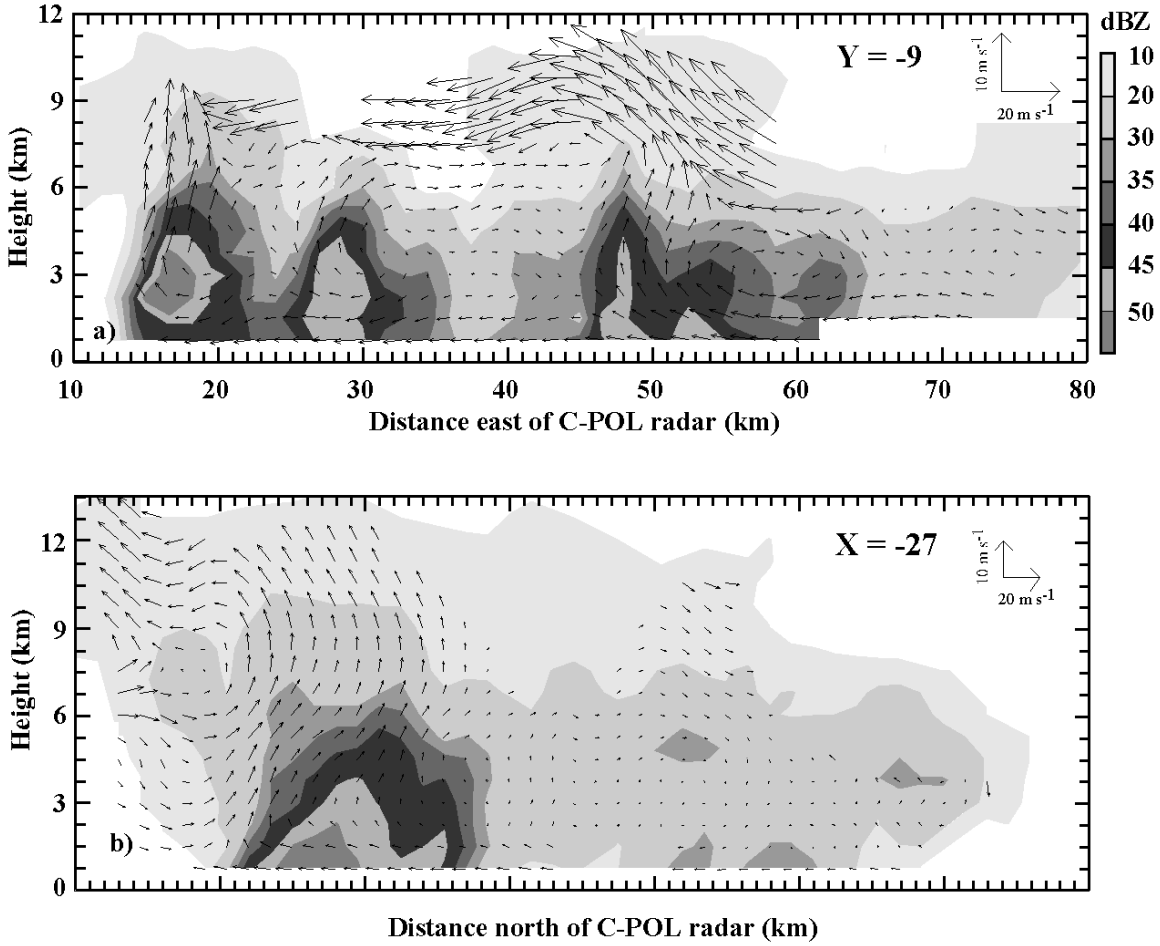

Fig. 3 Vertical cross section of reflectivity and line-normal system relative wind valid at a) 0620 UTC, and b) 0930 UTC.

the lowest levels with the maximum reflectivity recorded. However, in the pre-frontal region, the mean radar reflectivity had a higher decrease rate with the height in the layers below the freezing level. Above the freezing level, rapid decrease in reflectivity was found same as other tropical monsoon convection, suggesting a mild updraft in the convection. The post-frontal convection had a significant higher frequency of occurrence of intense echoes at the upper level, implying that the post-frontal convection would likely produce a higher rain rate. Comparing to the results from GATE and TAMEX, the mean radar reflectivity profile of the post-frontal convection was very similar to that documented in earlier studies. Obvious difference of system-relative winds existed at the upper levels for the pre- and post-frontal convection. For the pre-frontal convection, the convective driven outflows at the upper level were very strong. For the post-frontal convection, the system relative flows at the upper level consisted a relative weak front to rear winds over the large stratiform region and a relative strong rear to front winds over the small convective region. Strong low-level convergence had a higher probability of occurrence for the post-frontal convection. The post-frontal convection also had a deep 9 km convergence layer, comparing to only a 4 km convergence layer for the pre-frontal convection. Apparently, the low-level convergence generated by the northerly frontal flows and southerly monsoon flows in the post-frontal regime is more pronounced than the convergence produced by two branches of southwesterly flows in the pre-frontal regime. This also explains that the convection in the post-frontal region was much taller and more intense.

ACKNOWLEDGEMENTS

This research was sponsored by National Aeronautics and Space Administration (NASA) under TRMM Grants NAG5-9699.

REFERENCES

Lau, K.-M., and co-authors, 2000: Report of the field operations and early results of the South China Sea Monsoon Experiment (SCSMEX). *Bull. Amer. Meteor. Soc.*, **81**, 1261-1270.

LeMone, M. A., E. J. Zipser, and S. B. Trier, 1998: The role of environmental shear and thermodynamic conditions in determining the structure and evolution of mesoscale convective systems during TOGA COARE. *J. Atmos. Sci.*, **55**, 3493-3518.

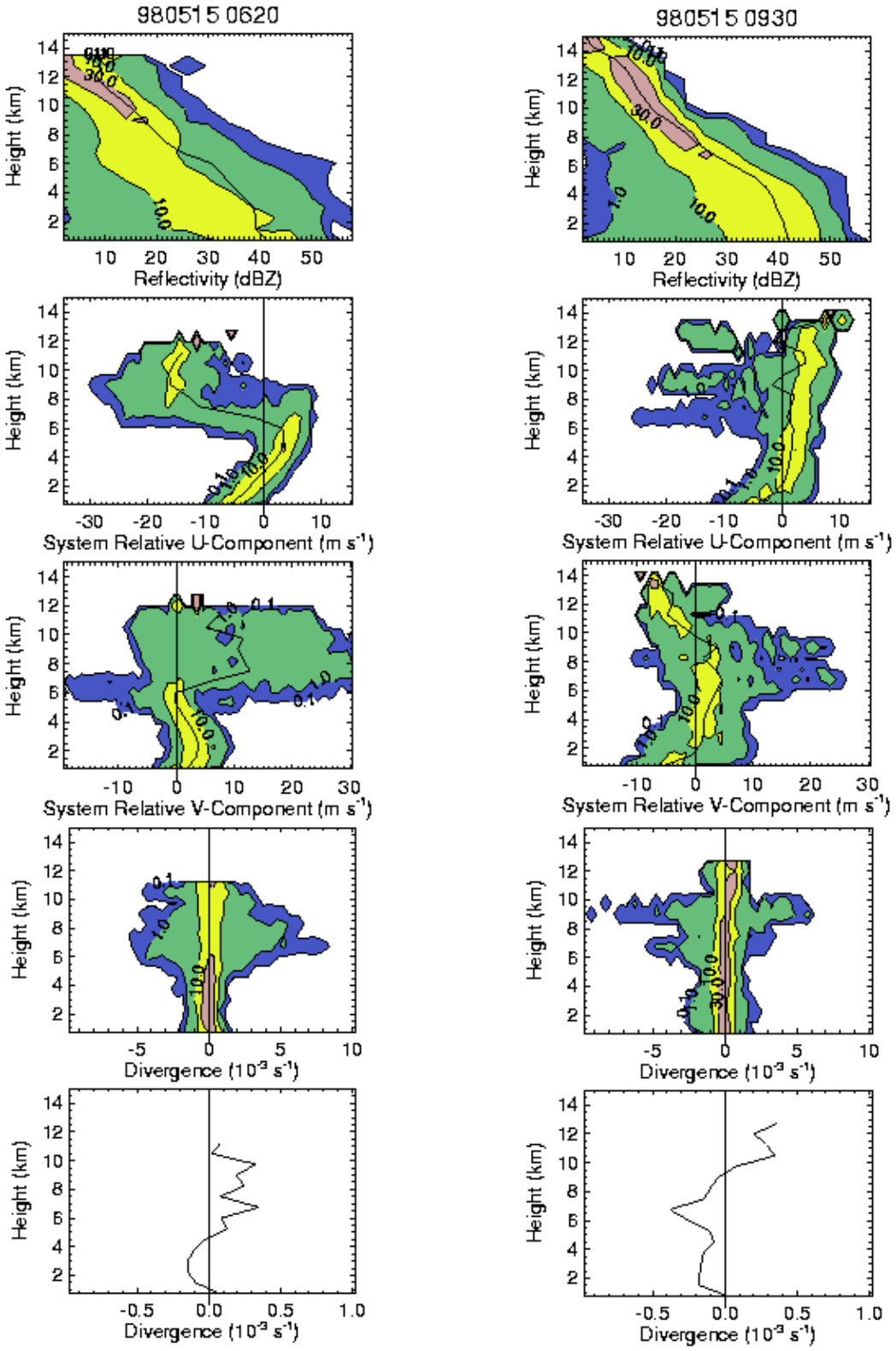

Fig. 4 CFADs and mean profiles of radar reflectivity, system relative u- and v-component, and divergence at 0620 UTC (left panels) and 0930 UTC (right panels) 15 May. Bin size is 4 dBZ for reflectivity, 1 m s^{-1} for u- and v-component, and 1×10^{-3} s^{-1} for divergence. Note the change in scale in the divergence CFADs and mean profiles.